

## Tailoring Lipoplex Composition to the Lipid Composition of Plasma Membrane: A Trojan Horse for Cell Entry?

Cristina Marchini,<sup>†</sup> Daniela Pozzi,<sup>‡</sup> Maura Montani,<sup>†</sup> Cinzia Alfonsi,<sup>†</sup> Augusto Amici,<sup>†</sup> Heinz Amenitsch,<sup>§</sup> Sofia Candeloro De Sanctis,<sup>‡</sup> and Giulio Caracciolo<sup>\*‡</sup>

<sup>†</sup>Department of Bioscience and Biotechnology, University of Camerino, Via Gentile III da Varano, 62032 Camerino (MC), Italy, <sup>‡</sup>First Faculty of Medicine, Department of Chemistry, 'Sapienza' University of Rome, P.le A. Moro 5, 00185 Rome, Italy, and <sup>§</sup>Institute of Biophysics and Nanosystems Research, Austrian Academy of Sciences, Schmiedelstrasse 6, A-8042 Graz, Austria

Received June 11, 2010. Revised Manuscript Received July 8, 2010

The first interaction between lipoplexes and cells is charge-mediated and not specific. Endocytosis is considered to be the main pathway for lipoplex entry. Upon interaction between lipoplexes and the plasma membrane, intermixing between lipoplex and membrane lipids is necessary for efficient endocytosis. Here we study the mechanism of the different endocytic pathways in lipid-mediated gene delivery. We show that DC-Chol-DOPE/DNA lipoplexes preferentially use a raft-mediated endocytosis, while DOTAP-DOPC/DNA systems are mainly internalized by not specific fluid phase macropinocytosis. On the other hand, most efficient multicomponent lipoplexes, incorporating different lipid species in their lipid bilayer, can use multiple endocytic pathways to enter cells. Our data demonstrate that efficiency of endocytosis is regulated by shape coupling between lipoplex and membrane lipids. We suggest that such a shape-dependent coupling regulates efficient formation of endocytic vesicles thus determining the success of internalization. Our results suggest that tailoring the lipoplex lipid composition to the patchwork-like plasma membrane profile could be a successful machinery of coordinating the endocytic pathway activities and the subsequent intracellular processing.

### Introduction

The success of gene therapy depends on the delivery of therapeutic gene to the designated target cells and their availability at the intracellular site of action.<sup>1</sup> Among nonviral gene delivery systems, synthetic cationic liposomes (CLs) are the most promising nonviral gene vectors.<sup>2</sup> When mixed with negatively charged DNA, CLs form stable complexes (lipoplexes) under equilibrium conditions. The most abundant nanoscale structure is the multilamellar liquid-crystalline phase<sup>3–5</sup> in which DNA chains are condensed between opposing cationic lipid membranes (Figure 1). The sandwiched DNA forms a one-dimensional (1D) array of chains which uniformly cover the available lipid area and the interhelical DNA–DNA distance,  $d_{\text{DNA}}$ , may range from approximately 25 Å where the DNA rods are nearly touching, to as large as about 55 Å.<sup>3</sup>

At present, the major disadvantage connected with the use of lipoplexes is their unsatisfactorily low transfection efficiency (TE) which depends on the poor understanding of their mechanism of transfection and the chemical and physical parameters of lipoplexes influencing it. Only a comprehensive knowledge of the interactions between lipoplexes and cells will result in optimization of TE. Early steps in the transfection process involve binding of the vector to the cell surface and its internalization inside the

cell cytosol (uptake).<sup>6–8</sup> It is generally accepted that interaction of lipoplexes with cells is nonspecific and involves mainly electrostatic interactions between the positively charged complexes and the negatively charged cell surface. Endocytosis is considered the main pathway for lipoplex entry, and different mechanisms have been described: caveolae-mediated endocytosis,<sup>9</sup> clathrin-mediated endocytosis,<sup>10</sup> caveolae- and clathrin-independent endocytosis,<sup>11</sup> and fluid-phase macropinocytosis.<sup>8,12,13</sup> The best characterized uptake mechanism is the clathrin-dependent pathway, which carries the lipoplexes into early and late endosomes that ultimately fuse with lysosomes and the trans-golgi network. The clathrin endocytic pathway involves the assembly of a specific coat protein, clathrin, on the intracellular face of the plasma membrane, resulting in the formation of a clathrin coated pit; this pathway is characteristic of receptor-mediated endocytosis. Treatments with substances that cause the dissociation of the clathrin lattice, i.e., chlorpromazine, can specifically inhibit clathrin-mediated endocytosis. Caveolae are invaginated, flask-shaped plasma membrane domains, which are especially enriched in cholesterol and sphingolipids.<sup>14,15</sup> Caveolae have been considered to be a specialized form of “lipid raft” domain with a unique morphology generated by caveolin, an integral membrane protein

\*E-mail: g.caracciolo@caspur.it.

- (1) Marshall, E. *Science* **2002**, *288*, 951–952.
- (2) Ramezani, M.; Khoshhamdam, M.; Dehshari, A.; Malaek-Nikouei, B. *Colloids Surf. B: Biointerfaces* **2009**, *72*, 1–5.
- (3) Radler, J. O.; Koltover, I.; Salditt, T.; Safinya, C. R. *Science* **1997**, *275*, 810–814.
- (4) Koltover, I.; Salditt, T.; Safinya, C. R. *Biophys. J.* **1999**, *77*, 915–924.
- (5) Caracciolo, G.; Caminiti, R. *Chem. Phys. Lett.* **2004**, *400*, 314–319.
- (6) Zuhorn, I. S.; Hoekstra, D. J. *Membr. Biol.* **2002**, *189*, 167–179.
- (7) Friend, D. S.; Papahadjopoulos, D.; Debs, R. J. *Biochim. Biophys. Acta* **1996**, *1278*, 41–50.
- (8) Prasad, T. K.; Rangaraj, N.; Rao, N. M. *FEBS Lett.* **2005**, *579*, 2635–2642.

- (9) Rejman, J.; Bragonzi, A.; Conese, M. *Mol. Ther.* **2005**, *12*, 468–474.
- (10) Zuhorn, I. S.; Kalicharan, R.; Hoekstra, D. J. *Biol. Chem.* **2002**, *277*, 18021–18028.
- (11) Hoekstra, D.; Rejman, J.; Wasungu, L.; Shi, F.; Zuhorn, I. S. *Biochem. Soc. Trans.* **2007**, *35*, 68–71.
- (12) Labat-Moleur, F.; Steffan, A. M.; Brisson, C.; Perron, H.; Feugeas, O.; Furstemberger, P.; Oberlong, F.; Brambilla, E.; Behr, J. P. *Gene Ther.* **1996**, *3*, 1010–1017.
- (13) Matsui, H.; Johnson, L. G.; Randell, S. H.; Boucher, R. C. *J. Biol. Chem.* **1997**, *272*, 1117–1126.
- (14) Rothberg, K. G.; Heuser, J. E.; Donzell, W. C.; Ying, Y. S.; Glenney, J. R.; Anderson, R. G. *Cell* **1992**, *68*, 673–682.
- (15) Deurs, B.; Roepstorff, K.; Hommelgaard, A. M.; Sandvick, K. *Trends Cell Biol.* **2003**, *13*, 92–100.

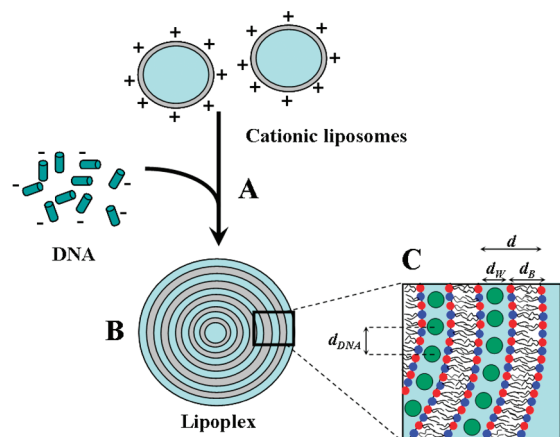


**Figure 1.** (A) Mixing of unilamellar cationic liposomes and DNA results in the spontaneous self-assembly of lipoplexes (B) with a multilamellar structure made of alternating lipid bilayers and water layers where DNA is confined. (C) Enlarged view of lipoplex structure showing characteristic distances at the nanoscale (cationic lipids in red, neutral lipids in blue).

directly interacting with cholesterol. Caveolae endocytosis is dependent on dynamin, which is localized to the neck of caveolae. Phosphorylation also plays an important role in caveolae budding: inhibition of tyrosine kinase activity blocks caveolae endocytosis.<sup>16</sup> Caveolae- and clathrin-independent endocytosis is mediated by cholesterol-rich microdomains. Fluid-phase macropinocytosis<sup>17</sup> is a triggered process used by the cell to internalize large amounts of fluid and membrane. Macropinocytosis is characterized by the formation of large, irregular primary endocytic vesicles after closure of ruffling membrane domains. Macropinosomes are dynamic structures that frequently move inward toward the center of the cell. Macropinocytosis is targeted by inhibiting phosphoinositide 3-kinase (PI3K), which is a key enzyme involved in phosphoinositide metabolism. Nowadays, it appears clear that a preferential endocytic pathway does not exist. It seems that the specific roles of different types of endocytosis in the uptake of lipoplexes depend on the lipoplex formulation as well as on the cell type. In recent papers, we have shown that structural and phase evolution of lipoplexes upon interaction with cellular membranes depend on the shape coupling between lipoplex and anionic membrane lipids.<sup>18,19</sup> We therefore hypothesized that the observed heterogeneity in the success and failure of a specific endocytosis mechanism is caused by regulatory mechanism that couples the lipid composition of lipoplexes and that of the cell surface.

The present work was intended to define the involvement of different endocytic pathways in lipid-mediated gene delivery and to assess a correlation between the routing mechanism of lipoplexes and their formulation. To this end, we investigated the mechanisms of uptake of three lipoplex formulations by treating NIH 3T3 cells with endocytosis inhibitors. The first two formulations were the widely used binary systems made of the combination of the cationic lipid 1,2-dioleoyl-3-trimethylammonium-propane (DOTAP) with the zwitterionic helper lipid dioleoylphosphocholine (DOPC) (DOTAP–DOPC), or of the cationic lipid

(3 $\beta$ -[*N*-(*N*′, *N*′-dimethylaminoethane)-carbamoyl]-cholesterol (DC–Chol) with the zwitterionic lipid dioleoylphosphatidylethanolamine (DOPE) (DC–Chol–DOPE). The third formulation was the multicomponent (MC) system obtained by mixing of the above-described binary formulations (DOTAP–DOPC–DC–Chol–DOPE). MC complexes were found to be highly efficient as a DNA delivery vector in comparison with the most common binary formulations used for transfection purposes.<sup>20,21</sup>

## Materials and Methods

**I. Liposomes Preparation.** Cationic 1,2-dioleoyl-3-trimethylammonium propane (DOTAP), dimethyldioctadecylammonium (bromide salt) (DDAB), [3 $\beta$ -[*N*-(*N*′, *N*′-dimethylamino)-ethyl]-carbamoyl]cholesterol (DC–Chol), zwitterionic dioleoylphosphatidylethanolamine (DOPE), and dioleoylphosphocholine (DOPC) were purchased from Avanti Polar Lipids (Alabaster, AL) and used without further purification. Binary DOTAP–DOPC and DC–Chol–DOPE CLs were prepared according to standard protocols.<sup>22</sup> In brief, binary mixtures, at molar fractions of neutral lipid in the bilayer  $\Phi$  = neutral lipid/total lipid (mol/mol) = 0.5 were dissolved in chloroform, and the solvent was evaporated under vacuum for at least 24 h. The obtained lipid films were hydrated with the appropriate amount of a Tris-HCl buffer solution ( $10^{-2}$  M, pH 7.4) to achieve the desired final concentration (10 and 1 mg/mL for SAXS and electrophoresis experiments, respectively). The obtained liposome solutions were stored at 30 °C for 24 h to achieve full hydration. Indeed, we have recently found evidence that lipid hydration is important to achieving the equilibrium structure of lipoplexes.<sup>22</sup>

**II. Lipoplexes Preparation.** For SAXS, DLS and  $\zeta$ -potential calf thymus (CT) Na-DNA, purchased from Sigma-Aldrich (St. Louis, MO), were used. CT Na-DNA was dissolved in Tris-HCl buffer (1 mg/mL) and was sonicated for 5 min inducing a DNA fragmentation with length distribution between 500 and 1000 bp, which was determined by gel electrophoresis. For transfection and electrophoresis experiments, plasmid DNA (pGL3 which codifies for firefly luciferase) (Promega, Madison, WI) was employed. The vector pGL3-control used in this study was transformed into *E. coli* strain DH5 $\alpha$  and grown in Luria–Bertani medium supplemented with ampicillin. The plasmid DNA was purified using a Maxiprep kit (Qiagen, Crawley, UK), and the concentration was determined spectrophotometrically at 260 nm.

By mixing adequate amounts of the DNA solutions to suitable volumes of liposome dispersions, self-assembled lipoplexes were obtained. All samples were prepared at a fixed cationic lipid/DNA charge ratio (mol/mol), i.e.,  $\rho$  = cationic lipid (by mole)/DNA (base) = 3. Such a value was chosen because it corresponds to the middle of a typical plateau region observed for optimal transfection conditions.<sup>20</sup>

**III. Luciferase Transfection Studies with Endocytosis Inhibitors.** Different endocytosis inhibitors were purchased from Sigma-Aldrich (St. Louis, MO). Fibroblasts NIH 3T3 were cultured in Dulbecco’s modified Eagle’s medium (DMEM) with Glutamax I (Invitrogen, Carlsbad, CA) supplemented with 10% fetal bovine serum (FBS) (Invitrogen) at 37 °C and 5% CO<sub>2</sub> atmosphere, splitting cells every 2–4 days to maintain monolayer coverage. Twenty four hours before transfection, 150 000 cells were seeded per well into 24-well culture plates, in order to reach 70–80% confluence

(16) Couet, J.; Sargiacomo, M.; Lisanti, M. P. *J. Biol. Chem.* **1997**, *272*, 30429–30438.

(17) Mandrekar, S.; Jiang, Q.; Lee, C. Y. D.; Koenigsnecht-Talboo, J.; Holtzman, D. M.; Landreth, G. E. *J. Neurosci.* **2009**, *29*, 4252–4262.

(18) Caracciolo, G.; Marchini, C.; Pozzi, D.; Caminiti, R.; Amenitsch, H.; Montani, M.; Amici, A. *Langmuir* **2007**, *23*, 4498–4508.

(19) Pozzi, D.; Caracciolo, G.; Caminiti, R.; Candeloro De Sanctis, S.; Amenitsch, H.; Marchini, C.; Montani, M.; Amici, A. *ACS Appl. Mater. Interface* **2009**, *10*, 2237–2249.

(20) Caracciolo, G.; Pozzi, D.; Caminiti, R.; Marchini, C.; Montani, M.; Amici, A.; Amenitsch, H. *Biochim. Biophys. Acta* **2007**, *1768*, 2280–2292.

(21) Caracciolo, G.; Caminiti, R.; Digman, M. A.; Gratton, E.; Sanchez, S. *J. Phys. Chem. B* **2009**, *113*, 4995–4997.

(22) Pozzi, D.; Amenitsch, H.; Caminiti, R.; Caracciolo, G. *Chem. Phys. Lett.* **2006**, *422*, 439–445.

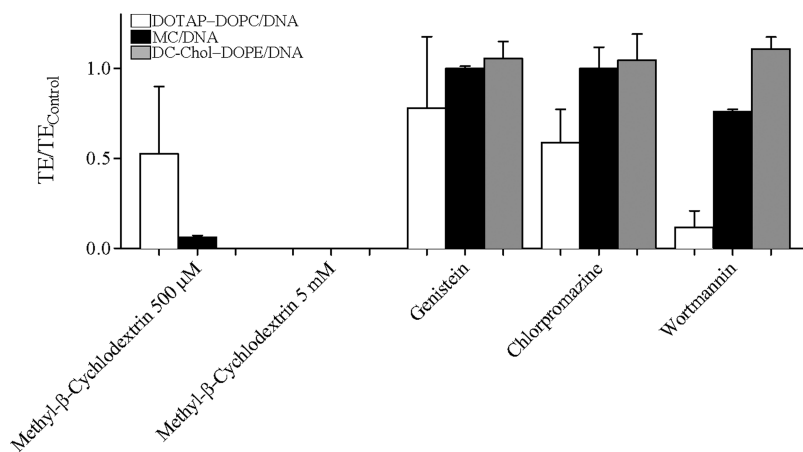


**Figure 2.** Effect of inhibition drugs on the transfection efficiency of lipoplexes. Complete inhibition indicates zero vertical value and thus the relative bar is invisible in the graph.

during transfection. Fibroblasts NIH 3T3 were pretreated with chlorpromazine (60  $\mu\text{M}$ ), wortmannin (10  $\mu\text{M}$ ), genistein (200  $\mu\text{M}$ ), and methyl- $\beta$ -cyclodextrin (500  $\mu\text{M}$  and 5 mM) in Optimem for 30 min prior to addition of lipoplexes to the cells. Inhibitor concentrations were chosen according to previous works.<sup>9,10</sup> Levels of proteins produced by treated cells were the same as those of untreated cells. This guaranteed that treating cells with inhibitors, at least at the concentrations used in the present study, did not result in any appreciable cell death. Lipoplexes were prepared in Optimem (Invitrogen) by mixing for each well of 24 well plates 0.5  $\mu\text{g}$  of plasmid with 5  $\mu\text{L}$  of sonicated lipid dispersion (1 mg/mL). These complexes were left for 20 min at room temperature before adding them to the cells. During transfection the cells were incubated in the presence of inhibitors (4 h at 37  $^{\circ}\text{C}$ ). Afterward, the cells were washed 3x with PBS before they were incubated in 1 mL of growth medium for 48 h. Finally, cells were washed in PBS and harvested in 200  $\mu\text{L}$  reporter lysis buffer (Promega, Madison, WI). A total of 20  $\mu\text{L}$  of cell suspension were diluted in 100  $\mu\text{L}$  luciferase reaction buffer (Promega) and the luminescence was measured 10 s using a luminometer (Berthold, Bad Wildbad, Germany). Results were expressed as relative light units per mg of cell proteins as determined by Bio-Rad Protein Assay Dye Reagent (Bio-Rad, Hercules, CA). Each experiment was performed in quadruple and repeated three times.

**IV. Agarose Gel Electrophoresis Experiments.** Electrophoresis studies were conducted on 1% agarose gel containing ethidium bromide in Tris-Borate-EDTA (TBE) buffer as elsewhere described.<sup>18</sup> Lipoplexes were prepared by mixing 5  $\mu\text{g}$  of DNA plasmid with 42  $\mu\text{L}$  of sonicated lipid dispersion (1 mg/mL). These complexes were left for 20 min at room temperature before incubating them in methyl- $\beta$ -cyclodextrin (500  $\mu\text{M}$  and 5 mM) for 4 h. Then, 10  $\mu\text{L}$  of lipoplexes were loaded on agarose gel. The electrophoresis gel was visualized and digitally photographed using a Kodak Image Station, model 2000 R (Kodak, Rochester, NY). Digital photographs (not reported) were elaborated using dedicated software (Kodak MI, Kodak) that allows calculation of molar fraction of free plasmid DNA (i.e., unprotected by lipids).

**V. Synchrotron Small Angle X-ray Scattering Measurements.** X-ray measurements were performed at the Austrian SAXS station of the synchrotron light source ELETTRA (Trieste, Italy).<sup>23</sup> SAXS patterns were recorded with two gas detectors based on the delay line principle. We investigated the  $q$ -range from  $q_{\min} = 0.05 \text{ \AA}^{-1}$  to  $q_{\max} = 0.6 \text{ \AA}^{-1}$  with a resolution

of  $5 \times 10^{-4} \text{ \AA}^{-1}$  (fwhm). The angular calibration of the detectors was performed with silver behenate powder  $d$ -spacing = 58.38  $\text{\AA}$ . The sample was held in a 1 mm glass capillary (Hildberg, Germany). The data have been normalized for variations of the primary beam intensity, corrected for the detector efficiency, and the background has been subtracted. Measurements were performed at 25  $^{\circ}\text{C}$ . The temperature was controlled in the vicinity of the capillary to within 0.1  $^{\circ}\text{C}$  (Anton Paar, Graz, Austria). Exposure times were typically 300 s. No evidence of radiation damage was observed in the X-ray diffraction patterns.

**VI. Size and  $\zeta$ -Potential Measurements.** All sizing and  $\zeta$ -potential measurements were made on a Zetasizer Nano ZS90 (Malvern, U.K.) at 25  $^{\circ}\text{C}$  with a scattering angle of 90 $^{\circ}$ . Sizing measurements were made on the neat vesicles dispersions, whereas the samples were diluted 1 in 10 with distilled water for the zeta potential experiments, to obtain reliable and accurate measurements. For all of the samples investigated, data show a unimodal distribution and represent the average of at least five different measurements carried out for each sample.

## Results

**I. Transfection Efficiency Experiments.** To define the mechanisms involved in the internalization and intracellular fate of lipoplexes, NIH 3T3 cells were pretreated before transfection with chemical agents that interfere with the various endocytotic pathways. Results presented in Figure 2 illustrate the effect of such drugs on the transfection activity mediated by lipoplexes made of DOTAP-DOPC/DNA (white bars), MC/DNA (black bars) and DC-Chol-DOPE/DNA (gray bars).

**Cholesterol Depletion.** First we verified if the transfection efficiency of binary and MC lipoplexes is dependent on cholesterol. To this end, methyl- $\beta$ -cyclodextrin, which is known to induce depletion of cholesterol from the plasma membrane, at two distinct inhibitor concentrations (500  $\mu\text{M}$  and 5 mM), was used. At 500  $\mu\text{M}$ , the percentage of inhibition did correlate with the molar fraction of DC-Chol in the membranes of lipoplexes. Transfection mediated by DC-Chol-DOPE/DNA lipoplexes was completely inhibited by the drug (50% DC-Chol in the lipid bilayer, 100% inhibition), this effect being less pronounced for MC/DNA (25% DC-Chol,  $\sim$  90% inhibition) and DOTAP-DOPC/DNA (0% DC-Chol,  $\sim$  70% inhibition) lipoplexes. Interaction of methyl- $\beta$ -cyclodextrin with unsaturated phospholipids present in the plasma membrane has been reported.<sup>24</sup> Thus, we asked whether the marked reduction

(23) Amenitsch, H.; Bernstorff, S.; Rappolt, M.; Kriechbaum, M.; Mio, H.; Laggner, P. *J. Synchrotron Radiat.* **1998**, *5*, 506–508.

(24) Puskas, I.; Csémpesz, F. *Colloids Surf. B: Biointerfaces* **2007**, *58*, 218–224.

in TE mediated by DC-Chol-DOPE/DNA lipoplexes could be due to neutral DOPE. To answer this question, the most obvious choice would have been substituting the cationic lipid DC-Chol with DOTAP. Unfortunately DOTAP-DOPE/DNA lipoplexes are prone to form hexagonal phases that have been hypothesized to enter cells via a fusion process.<sup>4</sup> To avoid misleading interpretation, DDAB-DOPE/DNA lipoplexes were used to transfect NIH 3T3 cells. DDAB is a cationic cylinder-like lipid and DDAB-DOPE/DNA complexes are assembled into liquid-crystalline lamellar phase. Cholesterol depletion did not affect DDAB-DOPE/DNA lipoplexes-mediated transfection (data not reported for space consideration). This finding suggests that the large reduction in TE mediated by DC-Chol-DOPE/DNA lipoplexes is mainly due to the presence of DC-Chol. The increase in the inhibitor concentration by 1 order of magnitude (5 mM) produced complete inhibition for all the lipoplex formulations. The latter finding can be easily explained bearing in mind that methylated cyclodextrins can interact with the membrane components of living cells causing irreversible changes in the physical stability and the permeability of the plasma membrane.<sup>24</sup> Such structural damages may ultimately lead to the disintegration of the cell membrane.

**Caveolae-Dependent Internalization.** Pretreatment of the cells with genistein, reported to block caveolae-mediated uptake processes,<sup>9,25</sup> prior to incubation with the lipoplexes had no significant effect on the uptake of DC-Chol-DOPE/DNA and MC/DNA lipoplexes. A more pronounced but minor inhibition effect was observed in the case of DOTAP-DOPC/DNA (less than 20% inhibition).

**Clathrin-Dependent Internalization.** Chlorpromazine, an inhibitor of clathrin-mediated endocytosis,<sup>9,26</sup> did not affect transfection mediated by DC-Chol-DOPE/DNA and MC/DNA lipoplexes. This finding led us to exclude the involvement of clathrin-dependent internalization for both these formulations. On the other hand, the inhibitor had a major effect on the transfection efficiency of DOTAP-DOPC/DNA systems (around 40% inhibition). These data are fully compatible with a major role of clathrin-mediated endocytosis in the internalization of DOTAP-rich lipoplexes. The predominant role of this mechanism in DOTAP-containing lipoplexes uptake was earlier reported.<sup>9</sup>

**Fluid-Phase Internalization.** Treatment of cells with wortmannin did not significantly perturb transfection efficiency of DC-Chol-DOPE lipoplexes, whereas it slightly reduced transfection mediated by MC lipoplexes (less than 20% inhibition). Most interestingly, wortmannin did inhibit DOTAP-DOPC gene delivery remarkably (about 80% inhibition). Therefore, the contribution of fluid-phase macropinocytosis seems to be determinant for DOTAP-DOPC-mediated cell transfection.

**II. Electrophoresis Results.** Among the drugs used in the present study, only methyl- $\beta$ -cyclodextrin can interact with the membrane components of living cells forming inclusion complexes. To exclude the possibility that methyl- $\beta$ -cyclodextrin may have interfered with cell transfection by altering the DNA-protection ability of lipoplexes, electrophoresis experiments on agarose gels were performed. In Figure 3, we present the digital photograph of DOTAP-DOPC/DNA lipoplexes pure (lane 1) and after a 4 h incubation of the lipoplexes with methyl- $\beta$ -cyclodextrin at two distinct concentrations (500  $\mu$ M, lane 2; 5 mM, lane 3). The experiment was replicated under the same experimental conditions with DC-Chol-DOPE/DNA formulations (lanes 4, 5, and 6).

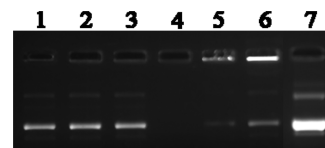


**Figure 3.** Digital photograph of DOTAP-DOPC/DNA lipoplexes in the absence of (lane 1) and after interaction with methyl- $\beta$ -cyclodextrin (500  $\mu$ M, lane 2; 5 mM, lane 3). The same experiment was replicated with DC-Chol-DOPE/DNA lipoplexes (lanes 4, 5, and 6). Lane 7 is control DNA.

Lane 7 is the control DNA. The high-mobility band was attributed to the most compact (supercoiled) form, whereas the less-intense one was considered to contain the nonsupercoiled content in the plasmid preparation. First, we observe that DC-Chol-DOPE/DNA lipoplexes exhibited a higher DNA-binding capacity (lane 4) than did DOTAP-DOPC/DNA lipoplexes (lane 1). Indeed, the digital photograph in Figure 3 points to the existence of a large amount of free DNA in the DOTAP-DOPC/DNA lipoplex formulation. The quantification of DNA (not reported) confirmed this observation. Approximately one-third of the DNA was found to be free and unprotected by DOTAP-DOPC cationic liposomes. The intensity of free DNA bands after incubation with methyl- $\beta$ -cyclodextrin (500  $\mu$ M, lane 2; 5 mM, lane 3) remained roughly the same as its counterpart in the inhibitor-free buffer (lane 1). Consequently, we conclude the DNA-binding ability of DOTAP-DOPC/DNA lipoplexes was not affected by incubation with methyl- $\beta$ -cyclodextrin. On the other side, the DNA-protection ability of DC-Chol-DOPE/DNA lipoplexes was largely modified by incubation with methyl- $\beta$ -cyclodextrin. Indeed, while pure lipoplexes protected all plasmid DNA (lane 4), free DNA was observed after incubation with methyl- $\beta$ -cyclodextrin ranging from less than 5% at 500  $\mu$ M (lane 5) up to about 20% at 5 mM (lane 6). This finding means that methyl- $\beta$ -cyclodextrin can promote DNA release from DC-Chol-rich lipoplexes. Noteworthy, a new band can be seen just below the wells after the incubation with methyl- $\beta$ -cyclodextrin whose intensity increases with increasing inhibitor concentration (lanes 5 and 6). We interpret the new band as plasmid DNA that is released from the lipid surface so that it is available to EtBr, but still confined by cationic lipid aggregates, so it cannot migrate very far from the wells.<sup>34</sup> Such DNA remains trapped within the confines of the lipid array but still protected by enzymatic attack.

**III. Synchrotron SAXS Results.** Synchrotron SAXS experiments clarified the structure of lipoplexes at the nanoscale. Representative SAXS patterns of DOTAP-DOPC/DNA, MC/DNA, and DC-Chol-DOPE/DNA lipoplexes are reported in Figure 4, panels a–c, respectively. All of the formulations formed highly organized lamellar phases (Figure 1). The sharp periodically spaced peaks at  $q_{0n}$  are caused by alternating lipid-bilayer-DNA monolayer structure with periodicity  $d = 2\pi/q_{001} = 64.5, 66.4,$  and  $68.5 \text{ \AA}$  for DOTAP-DOPC/DNA, MC/DNA, and DC-Chol-DOPE/DNA lipoplexes respectively. In Figure 4, the much broader peak marked by an arrow is the “DNA peak” arising from the one-dimensional 1D in plane lattice with repeat distance  $d_{\text{DNA}} = 2\pi/q_{\text{DNA}}$ . According to previous findings,<sup>27–29</sup> MC/DNA complexes have physical properties intermediate between those of binary ones.

(27) Caracciolo, G.; Pozzi, D.; Caminiti, R.; Amenitsch, H. *J. Phys. Chem. B* **2006**, *110*, 20829–20835.

(28) Caracciolo, G.; Pozzi, D.; Amenitsch, H.; Caminiti, R. *Langmuir* **2005**, *21*, 11582–11587.

(29) Caracciolo, G.; Pozzi, D.; Caminiti, R.; Amenitsch, H. *Appl. Phys. Lett.* **2005**, *87*, 133901.

(25) Rejman, J.; Oberle, V.; Zuhorn, I. S.; Hoekstra, D. *Biochem. J.* **2004**, *377*, 159–169.

(26) Vandenbroucke, R. E.; De Smedt, S. C.; Demeester, J.; Sanders, N. N. *Biochim. Biophys. Acta* **2007**, *1768*, 571–579.

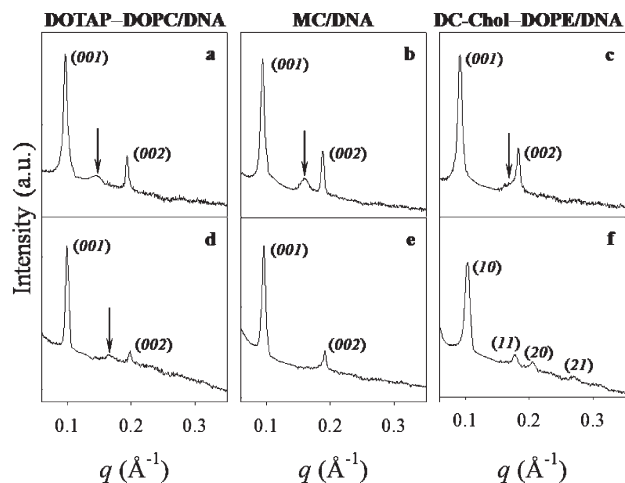


**Figure 4.** Representative SAXS patterns of DOTAP-DOPC/DNA (a), MC/DNA (b), and DC-Chol-DOPE/DNA (c) lipoplexes. Incubation with methyl- $\beta$ -cyclodextrin (500  $\mu$ M) produced changes in the SAXS patterns of DOTAP-DOPC/DNA (d), MC/DNA (e), and DC-Chol-DOPE/DNA (f) lipoplexes.

Recent studies showed that a critical factor in lipid-mediated transfection is the structural and phase evolution of lipoplexes upon interacting and mixing with cellular lipids.<sup>30–32</sup> Thus, to find out whether TE results may be due to destabilization of lipoplex nanostructure when in the presence of methyl- $\beta$ -cyclodextrin, SAXS experiments were replicated on the same samples after incubation with inhibitor (500  $\mu$ M) (Figure 4, panels d–f). Nanostructure of DOTAP-DOPC/DNA (Figure 4, panel d) was slightly affected by methyl- $\beta$ -cyclodextrin. The main effects were essentially two: (i) small, if any, enlargement in the lamellar  $d$ -spacing (less than 1 Å) and (ii) marked diminution of the 1D in-plane DNA order. The latter effect was clearly visible on the SAXS pattern where the DNA peak became weaker and broader. The interhelical DNA-DNA distance,  $d_{\text{DNA}}$ , is a very powerful tool that can be used to investigate the DNA release from lipoplexes upon interaction with lipids, detergents and other bilayer-destabilizing molecules.<sup>19</sup> Upon incubation with methyl- $\beta$ -cyclodextrin the DNA strands came closer as demonstrated by the DNA-DNA interdistance,  $d_{\text{DNA}}$ , that was found to decrease from 43.3 to 37.6 Å. According to recent publications, this suggests that DNA was not released from DOTAP-DOPC/DNA lipoplexes.<sup>19</sup> As evident, this result is in very good agreement with that achieved by electrophoresis (Figure 3) showing that the DNA-protection ability of DOTAP-DOPC cationic liposome was not affected by the inhibitor. If DNA is not released from lipoplex structure, the observed reduction in DNA-DNA distance is most likely to depend on the reduction in lipid membrane area available to 2D DNA condensation.<sup>33</sup> It is well-known that methylated cyclodextrins are able to extract lipids constituting cell membranes. Thus, the reduction in the interhelical DNA-DNA distance is compatible with a diminution of lipid membrane area most likely due to lipid removal from lipoplex lipid bilayer.<sup>34</sup> Similar results were obtained with MC/DNA lipoplexes (Figure 4, panel e). The initial lamellar structure

**Table 1.** Size,  $D$ , and Zeta-Potential,  $\zeta_p$ , of DOTAP-DOPC, MC, and DC-Chol-DOPE Cationic Liposomes Compared to DOTAP-DOPC/DNA, MC/DNA, and DC-Chol-DOPE/DNA Lipoplexes Prepared at the Cationic Lipid/DNA Molar Ratio  $\rho = 3$

	$D$ (nm)	$\zeta_p$ (mV)
DOTAP-DOPC	140 $\pm$ 1	51.4 $\pm$ 1.5
DOTAP-DOPC/DNA	234 $\pm$ 4	43.3 $\pm$ 1.5
MC	130 $\pm$ 4	53.2 $\pm$ 1.3
MC/DNA	205 $\pm$ 2	46.7 $\pm$ 1.2
DC-Chol-DOPE	110 $\pm$ 1	56.0 $\pm$ 1.3
DC-Chol-DOPE/DNA	180 $\pm$ 2	48.3 $\pm$ 1.2

of lipoplexes is almost unperturbed but short-range order in the DNA-DNA correlations is completely lost, as revealed by the disappearance of the “DNA peak” on the SAXS pattern.

On the other hand, the incubation of methyl- $\beta$ -cyclodextrin with DC-Chol-DOPE/DNA lipoplexes produced major structural modifications in the lipoplex structure. On the SAXS pattern (Figure 4, panel f) a new set of Bragg peaks was observed. They were indexed as the (10), (11), (20), and (21) reflections of a hexagonal phase with periodicity  $d = 70.2$  Å. This means that methyl- $\beta$ -cyclodextrin induced a lamellar-to-hexagonal phase transition in DC-Chol-DOPE/DNA lipoplexes. Methyl- $\beta$ -cyclodextrin is known to induce cholesterol depletion from membranes and a similar effect is expected to occur in DC-Chol-rich membranes.<sup>34</sup> As a result, upon DC-Chol removal from DC-Chol-DOPE mixed membranes, the spontaneous curvature of the monolayer mixture of DC-Chol and DOPE is driven negative by the increase in the relative percentage of curvature loving cone-like DOPE in the emerging lipid bilayer.

**IV. Size and  $\zeta$ -Potential Results.** The size and the  $\zeta$ -potential of DOTAP-DOPC, MC, and DC-Chol-DOPE cationic liposome formulations were examined by dynamic light scattering (Table 1). As evident, most vesicles are close to 100 nm in diameter and narrow particle size distributions ( $\text{pdi} < 0.2$ ) show liposome suspensions to be monodisperse. As expected, cationic liposomes exhibited very similar surface potential (Table 1). The size and the  $\zeta$ -potential of lipoplexes were also investigated to determine the importance of these parameters in transfection efficiency. DNA allowed CLs to come into contact and aggregate by reducing the intermembrane repulsive barrier essentially due to electrostatic repulsions. Upon charge neutralization, single lipid particles tend to stick when they collide because van der Waals short-range attractions can easily overcome weakened electrostatic repulsions. As a consequence, large aggregates formed (Table 1) with lipoplex size increasing from approximately 100 to more than 200 nm.

## Discussion

The transfection of cells by lipoplexes is a very complex process with a number of different stages.<sup>6,35,36</sup> For efficient optimization of the gene carrier it is important to profile its cellular uptake, because this largely determines its intracellular processing and subsequent transfection efficiency. Among specific barriers for transfection, cell uptake is thought to be rate-limiting but the current understanding of this process is still limited. Some authors showed that endocytosis of lipoplexes occurs through the cholesterol-dependent endocytosis pathway, while other groups provided evidence that the clathrin-mediated endocytosis was the most productive pathway for transfection. A size-dependent entry mechanism of lipoplexes has been recently proposed.<sup>25</sup> Particles

(30) Koynova, R.; Wang, L.; Tarahovsky, Y.; MacDonald, R. C. *Bioconjugate Chem.* **2005**, *16*, 1335–1339.

(31) Koynova, R.; Wang, L.; MacDonald, R. C. *Proc. Natl. Acad. Sci. U.S.A.* **2006**, *103*, 14373–14378.

(32) Koynova, R.; MacDonald, R. C. *Biochim. Biophys. Acta* **2007**, *1714*, 63–70.

(33) Caracciolo, G.; Pozzi, D.; Amici, A.; Amenitsch, H. J. *Phys. Chem. B* **2010**, *114*, 2028–2032.

(34) Piel, G.; Piette, M.; Barillaro, V.; Castagne, D.; Evrard, B.; Delattre, L. *Incl. Phenom. Macrocycl. Chem.* **2007**, *57*, 309–311.

(35) Medina-Kauwe, L. K.; Xie, J.; Hamm-Alvarez, S. *Gene Ther.* **2005**, *12*, 1734–1751.

(36) Dass, C. R. *J. Mol. Med.* **2004**, *82*, 579–591.

smaller than 300 nm should be mainly internalized through the clathrin-mediated pathway, whereas larger particles could enter the cells through caveolae. Lipoplexes used in the present investigation exhibited roughly the same diameter (Table 1) and their size was not found to correlate clearly with the mechanism of internalization. However, the size-dependent mechanism was demonstrated by using latex beads. When lipid vesicles are used, physical-chemical properties (such as lipid composition) other than size are expected to play a role in activating specific endocytic pathways.<sup>37</sup>

It is now clear that multiple endocytic pathways exist in mammalian cells and that their relative contribution depends either on the lipoplex formulation and on the cell type.<sup>37</sup> In recent publications,<sup>19</sup> we have demonstrated that structural and phase evolution of lipoplexes upon interaction with cellular membranes strictly depends on the shape coupling between lipoplex and anionic cellular lipids.

We hypothesize that the observed heterogeneity in the success and failure of a specific endocytosis mechanism in a given cell line could be affected by a regulatory mechanism that couples the lipid composition of lipoplexes and that of the cell surface. To evaluate this hypothesis, we investigated the effect of different endocytosis-interfering drugs (chlorpromazine, genistein, wortmannin, and methyl- $\beta$ -cyclodextrin) on the transfection efficiency of three selected lipoplex formulations. The widely used DOTAP–DOPC liposome formulations was chosen due to its liquid-crystalline phase of lipid bilayer that could promote favorable interaction with fluid-phase domains present in the plasma membrane. DC–Chol–DOPE formulation was chosen because it does contain DC–Chol, a cationic derivative of cholesterol, that is supposed to interact favorably with cholesterol-rich domains (i.e., caveolae and rafts) in the plasma membrane. The third system is the highly efficient MC system incorporating all the four lipid species. In Figure 2 we have shown that depletion of cholesterol from the plasma membrane inhibited functional delivery of plasmid DNA in the following order: DC–Chol–DOPE > MC > DOTAP–DOPC. These observations suggest that DC–Chol-rich complexes are internalized primarily by a cholesterol-dependent pathway. To exclude a simultaneous role played by the neutral helper lipid, the same experiment was replicated with DDAB–DOPE/DNA lipoplexes. We found that DDAB–DOPE/DNA-mediated transfection was not affected by cholesterol depletion.

From a structural point of view, synchrotron SAXS experiments showed that nanostructure of DOTAP–DOPC/DNA lipoplexes was slightly perturbed by methyl- $\beta$ -cyclodextrin (Figure 4, panel d). This finding was found to be in close agreement with electrophoresis findings showing that DNA was not released from lipoplexes (Figure 3, lane 2) after interaction with the inhibitor. On the other hand, the inhibitor induced a lamellar-to-hexagonal phase transition in DC–Chol–DOPE/DNA complexes (Figure 4, panel f). Hexagonal phase of lipoplexes has been reported to be more fusogenic than lamellar one and more prone to release DNA.<sup>4</sup> The latter evidence was in agreement with electrophoresis experiments (Figure 3, lane 5) showing that at 500  $\mu$ M of methyl- $\beta$ -cyclodextrin about 5% of DNA was released from hexagonal DC–Chol–DOPE/DNA complexes. The complexity of the multiple cholesterol-dependent endocytic pathways can be simplified by considering, at least, two distinct categories: caveolae-mediated and not caveolar raft-mediated endocytosis. To understand whether one of these two routes was predominant over the other, the effect of genistein, a caveolae-blocking drug, was evaluated. Figure 2 shows that neither DC–Chol–DOPE/DNA

nor MC/DNA lipoplexes were significantly inhibited by this inhibitor. A more pronounced effect was observed in the case of DOTAP–DOPC/DNA (less than 20% inhibition). This finding suggests that DC–Chol containing formulations are internalized via a not specific cholesterol-mediated route<sup>9</sup> but not significantly via caveolae, while the latter mechanism play some role for DOTAP–DOPC/DNA systems.

The role of fluid-phase macropinocytosis was investigated by treating cells with wortmannin. The precise role of this drug on endocytic activity of lipid-mediated transfection is under debate<sup>8</sup> and involvement of PI molecules in endocytosis, particularly in clathrin-coat-dependent processes, seems to be possible. However, it appears clear that wortmannin can inhibit fluid-phase macropinocytosis, a mechanism that is distinct from classic receptor-mediated endocytic pathways and does not involve membrane cholesterol. Figure 2 shows that this uptake mechanism does not play a significant role in DC–Chol-containing lipoplexes, while it seems to be determinant for DOTAP–DOPC-mediated cell transfection (80% inhibition).

Pretreatment of cells with chlorpromazine, an inhibitor of clathrin-mediated endocytosis, did affect neither DC–Chol–DOPE/DNA or MC/DNA lipoplexes mediated transfection. This finding led us to exclude major involvement of clathrin-dependent internalization for both these formulations. On the other hand, Figure 2 shows that chlorpromazine had a large effect on the transfection efficiency of DOTAP–DOPC/DNA systems (around 40% inhibition) suggesting that the clathrin-mediated endocytosis has a major role in the internalization of DOTAP lipoplexes. Our results are in very good agreement with previous findings showing the predominant role of this mechanism in DOTAP-containing lipoplexes uptake.<sup>9</sup>

As evident, our findings results the following body of evidence: (i) a specific lipoplex lipid composition could suppress one pathway, while being strongly required for the other and (ii) efficient MC lipoplexes do always exhibit an extent of inhibition intermediate between those of binary systems (Figure 2).

A number of recent findings have shown that the nanostructure of lipoplexes might change dramatically upon mixing with cellular lipids<sup>30–32</sup> and, furthermore, that such changes may critically affect transfection pathways and DNA delivery efficiency. The very first lipoplex–cell interaction is charge-mediated and not specific. Upon lipoplex–plasma membrane interaction, intermixing between lipoplex and membrane lipids is necessary for efficient endocytosis.<sup>38</sup> The plasma membrane itself is no longer considered a uniform structure but rather a patchwork of microdomains that can compartmentalize signaling.<sup>39</sup> Such domains are strongly regulated by lipid shape. The shapes of the volumes occupied by membrane lipids allow them to coordinately pack with other lipid types with “cognate” volume shapes, and this likely permits membrane curvature generation, a prerequisite for any endocytic pathway.<sup>38</sup> In recent publications,<sup>19</sup> we have shown that the propensity of lipoplexes to interact with cellular lipids does depend on the shape coupling between lipoplex and anionic membrane lipids. As a result, low packing competition between lipoplex and cellular lipids may result in the high incorporation efficiency of cellular lipids within lipoplex membranes. Thus, we suggest that such a shape-dependent coupling regulates efficient formation of endocytic vesicles thus determining the success of internalization.

The schematic reported in Figure 5 summarizes our present understanding of mechanisms occurring in the early stages of internalization of the lipoplex within the cell. Electrostatic attractions let

(37) Elouahabi, A.; Ruyschaert, J. M. *Mol. Ther.* **2005**, *11*, 336–347.

(38) Lakhan, S. E.; Sabharanjak, S.; De., A. J. *Biomed. Science* **2009**, *16*, 93.

(39) Mor, A.; Phillips, M. R. *Annu. Rev. Immunol.* **2006**, *24*, 771–800.

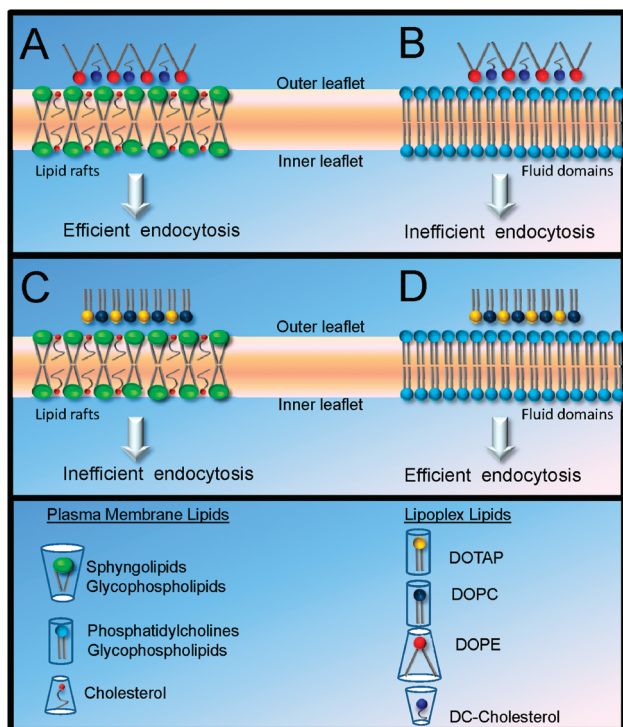


**Figure 5.** Proposed mechanism of the interaction of lipoplexes with the plasma membrane of the cell. Lipoplexes made of cholesterol-like lipids and cone-shaped lipids preferentially use lipid-rafts rich in cholesterol (A), whereas interaction with cylinder shaped membrane domains is inefficient (B). When lipoplexes made of cylinder-like fluid-phase lipids bind to lipid rafts (C), interaction is unfavorable and complexes accumulate at the plasma membrane, while binding to fluid microdomains results in efficient internalization (D).

the lipoplex approach the anionic surface of the cell made of lipid domains with size ranging from  $\sim 70$  nm to  $1 \mu\text{m}$ .<sup>40</sup> Since lipoplexes used in this study are about 200 nm in diameter, each lipid/DNA complex could interact with 1–2 lipid platforms. Shape coupling between lipoplex and membrane lipids regulate lipoplex–microdomain interaction thus determining the success of internalization along the specific pathway associated to the activated membrane domain. Thus, DC–Chol-rich lipoplexes could interact with lipid rafts where sphingolipids and cholesterol pack tightly excluding most phospholipids with unsaturated hydrocarbon tails. Only when the lipid/DNA particle encounters a region where it is

(40) Gupta, N.; DeFranco, A. L. *Mol. Biol. Cell* **2003**, *14*, 432–444.

able to bind multiple sterols simultaneously, for instance upon encountering a “lipid raft”, does it permanently bind and become trapped. This is in agreement with results of Figure 2 showing the reduction in TE produced by cholesterol depletion. For the same reason DOTAP–DOPC liquid-crystalline bilayers could favorably interact with fluid-phase domains that are richer in unsaturated lipids of similar shape. This is supported by the TE results obtained after treatment cells with wortmannin. On the other hand, DOTAP–DOPC/DNA lipoplexes could interact scarcely with “lipid rafts” remaining at the plasma membrane. This lipid shape-coupling model of interaction is supported by the results of recent fluorescent confocal experiments.<sup>21</sup> In time-dependent transfection efficiency experiments we have shown that maximum activity by lipoplexes was attained by 4 h of incubation. Confocal images of cells 4 h after incubation showed that transfection by two-component lipoplexes resulted in a distribution of intact complexes largely associated with the cell periphery.<sup>21</sup> On the other hand, confocal images of cells 4 h after incubation MC lipoplexes did not accumulate at the plasma membrane, but were almost completely internalized within cells.

Whatever the activated endocytic pathway is, MC lipoplexes did always exhibit an intermediate extent of inhibition (Figure 2). The latter observation suggests that MC systems can use multiple endocytic pathways to enter cells. This may therefore explain the superior efficiency of MC lipoplexes<sup>20,21</sup> with respect to binary ones used in the present study.

In summary, we have elucidated the uptake mechanisms responsible for the gene transfection of lipoplexes. Inhibition of specific endocytotic pathways did correlate with lipoplex lipid composition. Efficiency of endocytosis is regulated by shape coupling by lipoplex and membrane lipids. This indicates that tailoring the lipoplex lipid composition to the patchwork-like membrane profile could be a successful machinery of coordinating the endocytic pathway activities.

To bring lipoplexes to the forefront of gene delivery, in vivo application<sup>41</sup> is absolutely needed. To extend our conclusions to in vivo delivery, understanding to what extent the internalization mechanism is affected by the “protein corona”<sup>42–44</sup> dressed by lipoplexes in vivo is an urgent task. Future work will be performed in this direction.

(41) De la Torre, L. G.; Rosada, R. S.; Fávoro Trombone, A. P.; Frantz, F. G.; Coelho-Castelo, A. A. M.; Lopes Silva, C.; Andrade Santana, M. H. *Colloids Surf. B: Biointerfaces* **2009**, *73*, 175–184.

(42) Cedervall, T.; Lynch, I.; Foy, M.; Berggård, T.; Donnelly, S. C.; Cagney, G.; Linse, S.; Dawson, K. A. *Angew. Chem., Int. Ed.* **2007**, *46*, 5754–5756.

(43) Cedervall, T.; Lynch, I.; Lindman, S.; Berggård, T.; Thulin, E.; Nilsson, H.; Dawson, K. A.; Linse, S. *Proc. Natl. Acad. Sci. U.S.A.* **2007**, *104*, 2050–2055.

(44) Lynch, I.; Cedervall, T.; Lundqvist, M.; Cabaleiro-Lago, C.; Linse, S.; Dawson, K. A. *Adv. Colloid Interface Sci.* **2007**, *134–135*, 167–174.